Progress In Electromagnetics Research, PIER 92, 121–136, 2009

A PHOTON MODELING METHOD FOR THE CHARACTERIZATION OF INDOOR OPTICAL WIRELESS COMMUNICATION

H.-S. Lee

Department of Electronic Engineering
Sogang University
Seoul, Korea

Abstract—In this paper, an analysis method for optical wave propagation based on photon model is presented for the characterization of optical wireless communication environment. In contrast to radio waves, optical waves have very short wavelengths, so that material properties become important and often cause diffuse reflections. Channel models including diffuse reflections and absorption effects due to material surface textures make conventional electromagnetic wave analysis methods based on ray tracing consume enormous time. To overcome these problems, an analysis method using photon model is presented that approximates light intensity by density of photons. The photon model also ensures that simulation time is within a predictable limit and the accuracy is proportional to the number of total photons used in the simulation.

1. INTRODUCTION

A wireless communication system that uses visible light has many advantages with which it is possible to use very simple transmitter/receiver structures and easy to install; thus it receives much interest [1–4]. However, optical waves have very high frequency and their properties differ from conventional radio waves. In wireless radio communications, it is possible to build oscillators that have very long coherence time and use them to design coherent type modulation and demodulation circuits which accommodate high data rate communication with low signal to noise ratio (SNR), although the wireless terminals have somewhat complicated circuits that

Corresponding author: H.-S. Lee (leehs95@sogang.ac.kr).

raises manufacturing costs. In contrast to this, optical wireless communication terminals use simple light emitting diodes (LED) and photo transistor as a transmitter and receiver and it is possible to have very low cost terminals, while LED's very short coherence time prevents coherent modulation and necessitates high SNR.

The analysis of optical waves differs from radio waves in several aspects. In radio wave case, wavelengths are generally much larger than the surface roughness of the scattering objects and most of the reflections are of specular type and coherence of the waves is conserved. Diffractions are also important to radio waves in shadow region. In contrast, optical waves have very short wavelengths which are comparable or smaller than the surface roughness of the scatterers, and the reflected waves usually become diffusive. Surfaces that have random roughness generate diffuse reflections, and are called Lambertian surface. Random rough surfaces generate non-coherent waves after scattering and diffractions are ignored safely. Radio wave signals are received as voltages induced at the antenna port, while optical waves are recognized as photo currents generated in the photo-transistors which are proportional to the intensity of light. Because the light intensity does not contain phase information, detected signals in optical receivers are simple summation of the input signal if the light waves undergo multi-path scattering. However, the coverage of optical wireless communication is limited, because its diffraction area is very small and can not be used in non-line of sight area. To overcome these problems, Lambertian surfaces are considered to diffuse light waves into larger area. But the larger coverage area causes ever increased propagation losses more than radio wave cases, so that accurate channel modeling is needed to design optical wireless links.

The conventional approaches are based on the ray tracing techniques [3–5], which take the properties of optical waves into consideration. The method launches a bundle of rays in every direction in the space and tracks the ray paths. It takes reflections and transmissions on the materials into account and multiplies reflection and transmission coefficients on each scattering. The scattering processes go on until a predetermined number of reflections or transmissions are completed. If the propagation takes place in an indoor environment, the rays suffer from many reflections and transmissions on the obstacles, which increase the computation time exponentially as the order of scattering increases. To overcome these problems, ray methods that use Monte Carlo technique, which do not track every possible ray path but choose random direction on each scattering are proposed [6–9]. The technique reduces computational burdens in predicting an impulse response at one point, but it still

needs a lot of computations to analyze channel characteristics which need global simulation results at numerous reception points. The light illumination is also the research topic of the computer graphics field, where ray tracing techniques are developed to get high quality graphic images. Of those techniques, a photon map method [10] and its derivatives [11, 12] are developed and utilized to accelerate photo-realistic image generation process. In those techniques, light illumination phenomena are described by a number of photons stored on the surface of objects. The photons are stored when light waves hit objects with diffusing surfaces and are utilized in rendering images.

In this paper, the photon mapping method is imported and adapted to analyze optical wireless channel properties. In traditional ray tracing techniques, ray paths are bent or refracted on the surfaces of the obstacles according to Snell's law. But rays diffuse or split when they hit rough surfaces. The amount of computations increases exponentially as the ray spreads and goes on hitting multiple objects. Fig. 1(a) shows the situation when a light source emits rays in a box with Lambertian surfaces in a traditional ray tracing model. The arrows represent ray paths and they have weighting factor proportional to light intensities. In Fig. 1(b), the arrows represent photon paths of which densities represent light intensities which do not need any consideration for weighting factor. In this model, a light source is specified by the number of photons and an angular distribution of photons which is proportional to spatial light intensity.

For each photon, the angular direction of emission is chosen with the probability proportional to the radiation pattern of the light source. The emitted photon propagates until it hits an object. Then,

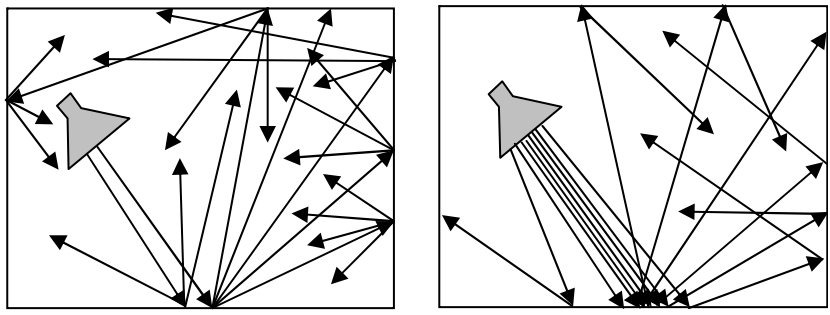

Figure 1. Ray paths by photon model and by simple ray tracing method when surrounding surfaces cause diffuse reflections.

the scattered direction is determined by the property of the surface. If the surface is specular, the direction is determined uniquely by the Snell's law. Whether it reflects or transmits into the surface is determined by the probability proportional to the reflectivity of the surface. If the surface is diffusive, the scattered direction of each photon is chosen with the probability proportional to the angular distribution function of scattered light which is inherent property of the surface. Whereas the number of ray directions in traditional ray tracing techniques increases on each diffuse reflection, the number of directions in which each photon scatters is only one that is chosen to satisfy the surface property statistically. Whenever a photon hits an obstacle, the direction of the photon is changed. If the surface is diffusive, all we have to do is choosing one scattered direction for each photon according to the distribution function of diffuse light. If the surface is lossy, photons are absorbed on the surface and do not continue scattering any longer. Whether a certain photon is absorbed or not is determined by the probability proportional to the reflectivity. In Fig. 1(b), photons first hit the bottom surface which is absorptive and the number of photons decreases after scattering. Secondly, photons hit the right wall of which texture is not absorptive and the number of photons is conserved after hitting. Because the surface is rough, the directions of scattered photons are random but follow the distribution function of scattered light statistically. The distribution function of scattered light is closely related to the surface property and has been studied in computer graphics, where the function is called the bidirectional reflectance distribution function (BRDF). The concept is utilized for optical wireless channel modeling in this paper. With photon model, the number of computations of photon scattering is at most a product of the number of initial photons and the order of reflections/transmissions, while the needed computations for the traditional ray techniques are exponentially proportional to the order. In the following sections, a calculation procedure for light intensities and a modeling method for the surface of obstacles are explained in detail.

2. ANALYSIS USING PHOTON MODEL

On using a photon method in optical wireless communication, three factors should be considered. They are light sources, changes in photon distributions after hitting obstacles, and parameter extraction techniques such as light intensity, impulse response, time delay, etc. Fig. 2 shows photons scattered at the object in an indoor environment. The spatial density of photons emitted from a light

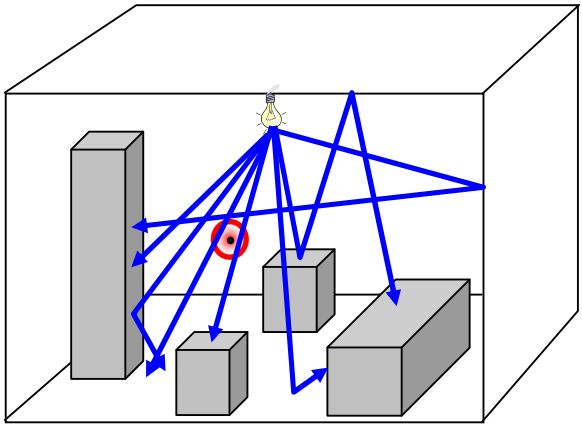

Figure 2. Photon paths emitted from a light source.

source follows a radiation pattern of the source, but it is changed after hitting the surface of obstacles. As the wavelengths of optical waves are comparable to the particles that form material surfaces, the distribution of photons after scattering depends on specific surface textures. If the distribution functions are tabulated by measured data or represented by simple parametric models, it is possible to predict optical wireless channel parameters accurately. If a surface is smooth with reflectivity less than unity, proportional photons are absorbed on scattering and the rest go on propagation in the direction that follows Snell's law. In case of a diffusive surface, outgoing photons distribute themselves following the BRDF of the surface. As the photons propagate, their densities in space decrease with longer traversed distances. Utilizing these properties, a numerical prediction of optical wireless channel characteristics is possible. In Sections 2.1, 2.2, 2.3, methods are presented for modeling light sources, material surface textures, and light intensities, and delay profiles of optical signals. In Section 2.4, a modeling method for receiver characteristics is dealt with.

2.1. Modeling of Light Source

Properties of light sources can be modeled by spectrum information and radiation patterns. As light sources generate photons, two kinds of information are needed. They are the spectrum and radiation patterns of the sources. As the light intensity is calculated from photon density, the spectral and spatial distributions of photons should follow the specified power spectrum and pattern of the light source.

Two random numbers are used to generate photons which statistically follow the predetermined distribution functions. One random number is generated and mapped into wavelengths, and the other is to simulate distribution in spatial domain. If an accurate simulation result is required, the number of photons should be increased to reduce sampling noises.

To generate random numbers using a computer code, a C++ compiler library function "rand()" is used which generates an arbitrary integers ranged from 0 to RANDMAX (32767). The random integers become seeds of a wavelength and photon direction selection routine that follows prescribed distribution functions. In the selection process, rejection method [12] of Monte Carlo simulation is utilized. Fig. 3 shows how to generate random number x that conforms to distribution function $f(x)$. To generate a photon with a specific wavelength, the rejection method generates a random number pair (x_1, y_1) using rand() function. If the pair satisfies $y_1 < f(x_1)$, a photon with a wavelength x_1 is generated. If not, random number generation process is tried again until the condition is met. With this selection process, photons with distribution function $f(x)$ are obtained.

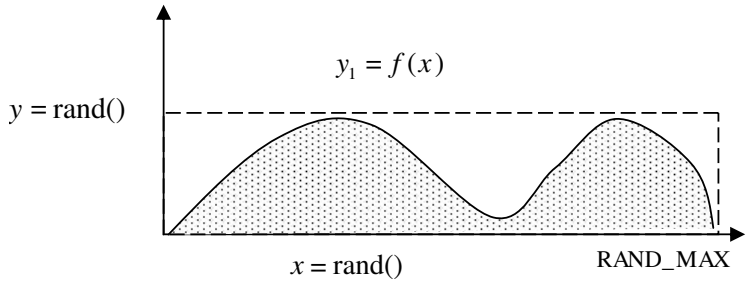

Figure 3. A method of photon generation which conforms to an arbitrary distribution function $y = f(x)$.

To model a spatial distribution of photon directions, the previous one dimensional rejection test for wavelength is extended to a two-dimensional selection procedure. That is, photon directions are arbitrarily chosen of which distribution function is the radiation pattern of the light source. If the radiation pattern is $f(\theta, \varphi)$, a random number pair (θ_1, φ_1) is chosen such that $y_1 < f(\theta_1, \varphi_1)$ is satisfied.

2.2. Reflections and Transmissions of Photons

The direction of a propagating photon is changed upon colliding with obstacles. The outgoing direction of the photon is chosen with

probability that depends on the specific material property, incident direction, etc. The probability function is proportional to scattered light intensity distribution function which can be obtained from BRDF of the surface. The BRDF can be measured by a goniometer and is related to the texture of a specific material surface.

The scattered direction of a photon is determined statistically using BRDF which is widely used in computer graphics. The choice of direction is performed by the same rejection test as used for modeling a light source pattern. But the definition of BRDF used in computer graphics is made for the quantity of radiance. To paraphrase BRDF for photon density, the scattered photon density in the direction of $\vec{\omega}$ is as follows.

$$\frac{d\Phi_r}{d\omega_r} = f_{\text{BRDF}} \cos\theta_r \cdot d\Phi_i \tag{1}$$

where Φ_i and Φ_r represent an incident photon density and that of reflected photons. θ_r is the angle between the surface normal vector and a reflected direction. The BRDF is obtained from measurement data and utilized in tabulated or parametric function form. In this paper, the BRDF of Schlick's [14] is utilized which has polynomial form for rapid calculation. Schlick's BRDF of a surface x is as follows.

$$f_{BRDF}(x, \vec{\omega}, \vec{\omega}') = S(u) \left\{ \begin{array}{l} \frac{d}{\pi} + gD\left(t, \upsilon, \upsilon', w\right) \\ +sf_{r,s}\left(x, \vec{\omega}, \vec{\omega}'\right) \end{array} \right\} \tag{2}$$

where $S(u)$ is a reflectivity which is equal to the square of Fresnel reflection coefficient of the surface, and $u = \vec{\omega} \cdot \hat{H}$, $t = \hat{\mathbf{n}} \cdot \hat{H}$, $\upsilon = \vec{\omega} \cdot \hat{\mathbf{n}}$, $\upsilon' = \vec{\omega}' \cdot \hat{\mathbf{n}}$, $w = \overline{H} \cdot \hat{T}$. $\vec{\omega}$ stands for the direction of scattered photon, and $\vec{\omega}'$ that of incident photon. The three terms in the parenthesis stand for Lambertian, directional diffuse, and specular reflections, respectively. The factors d, g, and s represent the relative contribution of each reflection type. In [14], $\vec{\omega}'$ is defined as an opposite direction of the incident photon. The normal vector of the surface is $\hat{\mathbf{n}}$. $\hat{H}, \overline{H}$ and $\hat{T}$ are defined as the following equations.

$$\hat{H} = \frac{\vec{\omega} + \vec{\omega}'}{|\vec{\omega} + \vec{\omega}'|}, \quad \hat{T} = \frac{\vec{\omega}' \times \hat{\mathbf{n}}}{|\vec{\omega}' \times \hat{\mathbf{n}}|}, \quad \overline{H} = \frac{\hat{H} - (\hat{\mathbf{n}} \cdot \hat{H})\hat{\mathbf{n}}}{\left|\hat{H} - (\hat{\mathbf{n}} \cdot \hat{H})\hat{\mathbf{n}}\right|} \tag{3}$$

The symbol $\hat{H}$ represents a unit vector parallel to the bisector of $\vec{\omega}'$ and $\vec{\omega}$. $\vec{T}$ is a direction perpendicular to both $\vec{\omega}'$ and $\hat{\mathbf{n}}$. After Schlick's definitions, the remaining symbols are as follows. The directional diffuse term is defined to be

$$D(t, \upsilon, \upsilon', w) = \frac{G(\upsilon)G(\upsilon')Z(t)A(w) + 1 - G(\upsilon)G(\upsilon')}{4\pi\upsilon\upsilon'} \tag{4}$$

$$Z(t) = \sigma[1 + (\sigma - 1)t^2]^{-2}, \quad A(w) = \sqrt{\frac{\psi}{\psi^2 - \psi^2 w^2 + w^2}},$$
$$G(\upsilon) = \frac{\upsilon}{\sigma - \sigma\upsilon + \upsilon} \tag{5}$$

$$g = 4\sigma(1-\sigma),\ d = \begin{cases} 0 & \text{for } \sigma < 0.5 \\ 1-g & \text{otherwise} \end{cases},\ s = \begin{cases} 1-g & \text{for } \sigma < 0.5 \\ 0 & \text{otherwise} \end{cases} \tag{6}$$

The above equations are introduced to approximate the experimentally determined BRDF by simple polynomial functions. For Schlick's model, two parameters should be experimentally determined. They are roughness (σ) and anisotropy (ψ) of the surface. Their values ranges from 0 to 1. If the roughness is 0, the surfaces are perfectly smooth. With the roughness 1, the surface is Lambertian. With the anisotropy ψ is 1, the density of the reflected photons from the surface is isotropic, while with ψ zero, it is anisotropic. Using anisotropy, the textures of wood or metal are modeled. The direction of a scattered photon is determined by the same rejection method derived in the previous section. If an incident photon hits a surface, a random direction is selected among vectors pointing a hemispherical surface. Then, the BRDF is calculated with that direction and its value is used for a rejection test. If the direction is allowed, the outgoing photon is allowed to propagate in that direction. If not, another random direction is generated and is tried for the test again. With the procedure, optical properties of the surface are taken into consideration statistically.

2.3. Calculation of Light Intensity

Photons generated by light sources undergo scattering and their paths are kept in computer memory until they are absorbed in the surfaces of obstacles or the number of reflections/transmission exceeds a predetermined number. For all the photons, the procedure is reiterated and a set of photon paths is completed. With photon paths in memory, physical parameters such as light intensity, impulse response, and time delay profiles can be extracted.

To extract light intensity at a certain point, the number of photons that cross the position should be counted. With discrete photon paths in computer memory, it is difficult to figure out them. To get an approximate number, the concept of a reception sphere is adopted [15]. To calculate light intensity at an observation point, a sphere is formed whose center is located at the point, and intersections with the existing photon paths are examined. A photon path that comes into the sphere is counted as a received power. As the light intensity is a

power flux per unit area, it is calculated by the number of photons divided by the cross section area of the sphere. With the radius of the reception sphere small, a high resolution spatial distribution of light intensity is obtained, but due to the discrete nature of photon paths the distribution should have noises due to sampling and quantization. To get a more smooth spatial distribution, a sphere with larger radius is to be used. With larger radius, the spatial resolution is worse. For a high resolution intensity map with less noise, the number of photons should be increased with the radius of a reception sphere decreased.

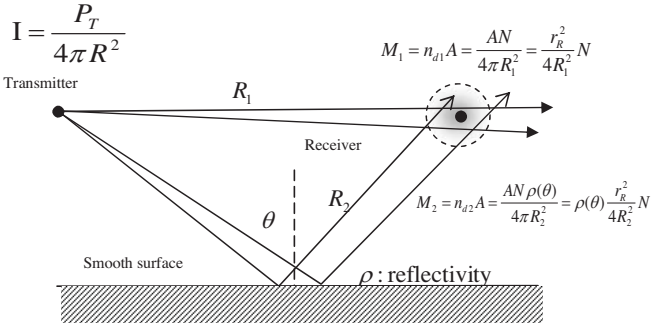

Figure 4. Calculation of light intensity using reception sphere.

Figure 4 explains how the densities of photon paths change with distance. Let the power emitted from a light source be P_t and the number of photons be N. If their directions are isotropic, the number of photons along the path R_1 that cross a surface with area A at the position of the receiver is given by Eq. (7).

$$M_1 = n_{d1}A = \frac{AN}{4\pi R_1^2} = \frac{r_R^2}{4R_1^2}N \tag{7}$$

It is clear that the density is inversely proportional to the square of the distance from the source, which is identical to the prediction by Maxwell's equations. The received power from the photons along the path R_1 is obtained by multiplying Eq. (7) and a power carried by one photon and is given in the following Eq. (8).

$$P_{R1} = M_1\frac{P_T}{N} = \frac{r_R^2}{4R_1^2}N\frac{P_T}{N} = \frac{r_R^2}{4R_1^2}P_T \tag{8}$$

If photons hit a surface with reflectivity ρ, the number of photon reflected from the surface is reduced by a factor of ρ. The contribution

of power along the path R_2 will be given in the following Eq. (9).

$$P_{R2} = \rho(\theta)\frac{r_R^2}{4R_2^2}P_T \tag{9}$$

where θ is the angle between the incident direction and the normal vector of the surface. R_2 is the total traversed distance from the source to the receiver by way of the hitting point at the surface, which is equal to the distance from the image source to the receiver position.

With photon paths in a computer memory, the total traversed distance of each photon from the source is easily calculated, which gives time delay information. To expedite calculation, various space partition methods such as octree, quad tree and acceleration techniques can be used [16–24]. The information is statistically analyzed and various channel parameters are obtained.

2.4. Receiver Property

The preceding power calculations do not include the properties of a receiver. Its properties are to be considered for realistic simulations. For receiver modeling, two factors are needed — the sensitivity function of wavelengths and its radiation pattern. The photo current of the receiver is given by Eq. (10)

$$I = \frac{1}{\pi r^2}\sum P_{\text{photon}} \cdot f_{\text{spectrum}}(\lambda) f_{\text{pattern}}(\hat{d}_{\text{photon}}) \tag{10}$$

where r is the radius of a reception sphere and $\hat{d}_{\text{photon}}$ is the direction of an incoming photon. The functions can be made from measurement data or datasheets from the manufacturer of photo transistor.

3. NUMERICAL CALCULATIONS

Using the proposed photon model, calculations are performed to compare the result by the photon model with existing data [1], where a point source is located in a room with dimension $5\,\text{m} \times 5\,\text{m} \times 3\,\text{m}$. The environment is tessellated into triangles of which surface texture data are included in them. Fig. 5 shows a result obtained by 2 million photons, which shows good agreement. The first peak is due to the power through the line of sight path. The result in [1] is obtained by a conventional ray tracing technique in which diffused rays are generated to every possible grid point of surrounding surfaces. In photon model, only one direction per photon is chosen on each reflection, but the collective behavior of photons agrees with [1] statistically. Due to the

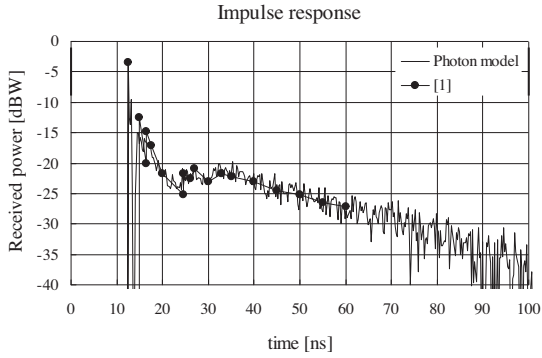

Figure 5. Comparison of simulation data with a result in [1]. An impulse response is plotted versus time delay. The x-axis is elapsed time after emission from the light source.

discrete nature of photons, the shape of the impulse response curve has a lot of noise like ripples. In the simulation, a light source and a receiver with cosine shape radiation pattern with 1 W are used. Walls and ceilings are lined with Lambertian textures with reflectivity 0.8. The floor is also a Lambertian surface with reflectivity 0.3. The photon method consumes much less time because the only operation needed is generating photons and counting them. With 2 million photons and the number of reflection 8, it takes only one minute to form photon paths in computer memory (CPU Intel core2duo 2.4 GHz). But the required time increases as the number of objects in the room increases. Fig. 6 shows the increase in simulation time as the order of reflections changes. With the reflectivities of walls and floor less than unity, the number of photons decreases as they undergo reflections. If the reflectivity is unity, the curve in Fig. 6 would be linearly proportional to the number of reflections.

Photons that follow statistically spectral and spatial distributions of a light source are generated and undergo reflections and transmissions to a prescribed order. Their paths are all kept in memory and utilized to extract communication parameters. Fig. 7 shows the result of an indoor environment furnished with a sofa and a table. A light source is located southeast of the room on ceiling. The number of photons is 1 million. Reflectivities of walls, floors, and the ceiling are all set to 0.44 and it is assumed that $\sigma = 0$ and $\psi = 1$. The figure shows a general trend that light intensity decreases with distance and delay spread increases. The delay spread is defined as the following

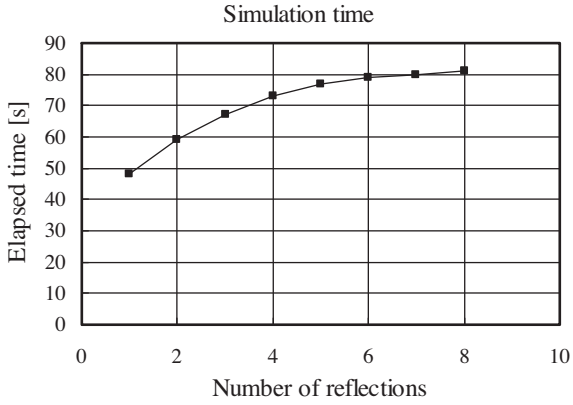

Figure 6. Sin the total elapsed time with the number of reflections changed. The number of emitted photons from the light source is three million. The environment is the same as the case of Fig. 5.

Eq. (11).

$$\tau = \sqrt{\frac{\sum_{i}^{n}(t_i - \overline{t})^2 P_i}{\sum_{i}^{n} P_i}} = \frac{1}{c}\sqrt{\frac{\sum_{i}^{n}(l_i - \overline{l})^2}{n}}, \qquad (11)$$

$$\overline{t} = \left(\sum_{i}^{n} t_i P_i\right) \Big/ \left(\sum_{i}^{n} P_i\right) = \left(\sum_{i}^{n} l_i\right) \Big/ (cn)$$

where P_i is the received power of i-th photon which arrives at the receiver after the delay time t_i, and l_i is the total traversed distance from the light source. n is the number of photon paths that intersect a reception sphere and c is the speed of light. $\overline{t}$ and $\overline{l}$ are the average delay time and the average path length from the source, respectively. For each photon path, its total traversed distance is divided by the speed of light. Then, it is the time delay of that photon. If the time delay of each photon is added together and divided by the number of photon paths in the reception sphere, an average time delay is obtained. Likewise, the standard deviation of time delays of photons is obtained, which is equal to a delay spread at a receiving point. Fig. 7(c) shows a two dimensional delay spread distribution on the observation plane at the height of 30 cm from the floor. Delay spreads are calculated on 90,000 points and are plotted.

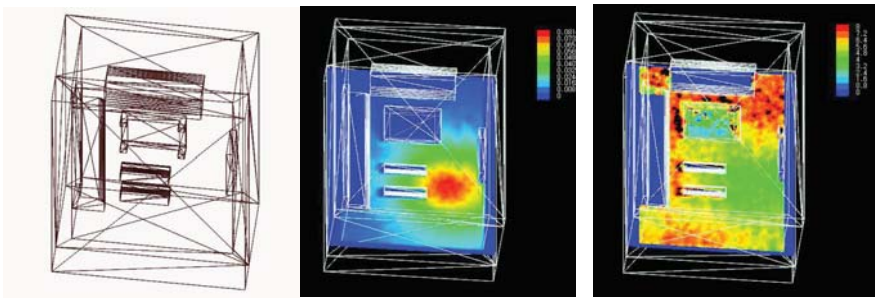

(a) (b) (c)

Figure 7. Simulation results of a room with sofas and a table. (a) indoor environment (b) distribution of light intensity (c) delay spread.

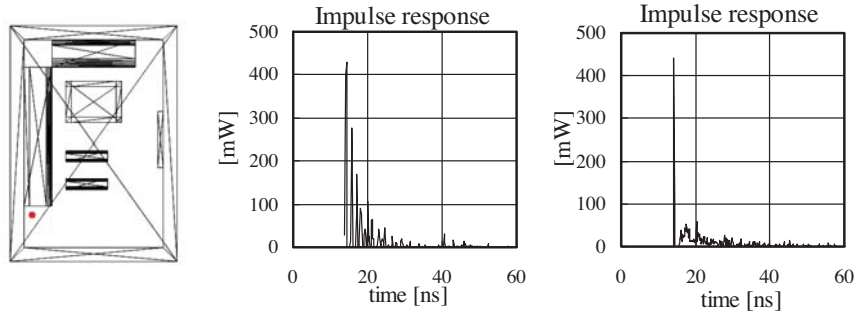

(a) (b) (c)

Figure 8. Impulse responses at a point marked by a small circle located at bottom left side. (a) observation point. (b) with specular surfaces. (c) with Lambertian surfaces.

Fig. 8(b) shows an impulse response observed at the bottom left position marked by a spot. When the surfaces are smooth and the texture is specular, the angular density of photons changes little even after they undergo many reflections. The spatially concentrated photon distributions make possible persistent temporal spread of photons. The density of photons decreases inversely proportional to the distance squared. Fig. 8(c) shows a response after the textures of floor, sofas, ceilings are changed to be Lambertian. Compared with Fig. 8(b), the power delay profile rapidly converges to zero. With Lambertian surfaces, photons are spread widely on each reflection and the density of them decreases exponentially with the number of reflection. Their temporal distribution cannot be sustained long enough, so that the impulse response quickly becomes zero.

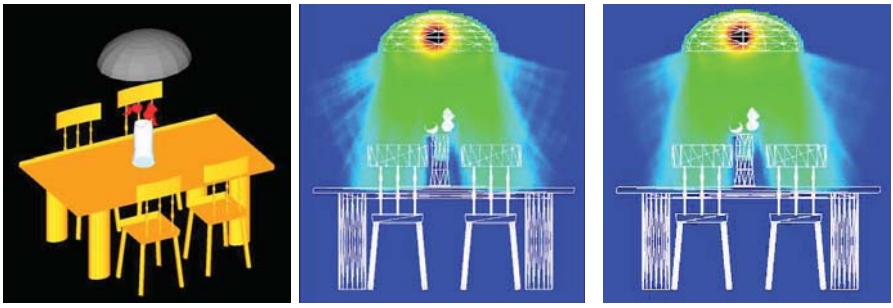

(a) (b) (c)

Figure 9. Simulation result of a set of a table and chairs illuminated by a light source with a reflector. (a) environment (b) intensity distribution with 100,000 photons. (c) result with 500,000 photons.

It can be seen that results of photon model rapidly converges in comparison with conventional ray tracing methods. Fig. 15 shows a more complex indoor situation, where a table, four chairs, a vase and a light source exist. The results are obtained with 100 thousand photons and with 500 thousand ones. The intensity distributions of the two cases are almost identical.

4. CONCLUSION

An analysis method for optical waves propagating in an indoor environment is proposed. The textures of objects should be taken into account when the wavelength of electromagnetic wave like optical waves is comparable to surface roughness. Scattering of the photons on surfaces with a specific texture is modeled by BRDF. To characterize an optical wireless channel, photon paths are stored in a computer memory. Using the photon paths, it is shown that light intensity can be calculated by counting photons intersecting a reception sphere that enclose an observation point. The photon model has an advantage that computation times increase linearly with the number of reflections. Methods for modeling light sources and receiver characteristics are also presented. Numerical computation shows that results obtained by photons show good agreement with existing results. Impulse responses with various indoor environments are also calculated with different texture parameters.

REFERENCES

1. Kahn, J. M. and J. R. Barry, "Wireless infrared communications," *Proc. IEEE*, Vol. 85, 265–298, 1997.
2. Komine, T. and M. Nakagawa, "Fundamental analysis for visible-light communication system using LED lights," *IEEE Trans. on Consumer Electronics*, Vol. 50, No. 1, 100–107, Feb. 2004
3. Barry, J. R., J. M. Kahn, W. J. Krause, E. A. Lee, and D. G. Messerschmitt, "Simulation of multipath impulse response for indoor wireless optical channels," *IEEE Journal on Selected Areas in Communications*, Vol. 11, No. 3, 367–379, Apr. 1993.
4. Kahn, J. M., et al., "Non-directed infrared links for high-capacity wireless LANs," *IEEE Personal communications*, No. 2, 1994.
5. Kahn, J. M., W. J. Krause, and J. B. Carruthers, "Experimental characterization of non-directed indoor infrared channels," *IEEE Trans. on Communications*, Vol. 43, No. 2, 1613–1623, Feb. 1995.
6. Lopez-Hernandez, F. J., R. Perez-Jimenez, and A. Santamaria, "Modified Monte Carlo scheme for high efficiency simulation of the impulse response on diffuse IR wireless indoor channels," *Electronics Letters*, Vol. 34, No. 19, 1819–1820, Sept. 1998.
7. Lopez-Hernandez, F. J., R. Perez-Jimenez, and A. Santamaria, "Ray tracing algorithms for fast calculation of the channel impulse response on diffuse IR wireless indoor channels," *Optical Engineering*, Vol. 39, No. 10, 2775–2780, Oct. 2000.
8. González, O., S. Rodrguez, R. Pérez-Jiménez, B. R. Mendoza, and A. Ayala, "Error analysis of the simulated impulse response on indoor wireless optical channels using a Monte Carlo-based ray-tracing algorithm," *IEEE Trans. on Communications*, Vol. 53, No. 1, 199–204, Jan. 2005.
9. Cocheril, Y. and R. Vauzelle, "A new ray-tracing based wave propagation model including rough surfaces scattering," *Progress In Electromagnetics Research*, PIER 75, 357–381, 2007.
10. Jensen, H. W., "Global illumination using photon maps," *Eurographics*, Vol. 7, 21–30, 1996.
11. Zinke, A. and A. Weber, "Efficient ray based global illumination using photon maps," *International workshop on Vision, Modeling, and Visualization*, 113–120, 2006.
12. Havran, V., J. Bittner, and H.-P. Seidel, "Ray maps for global illumination," *Eurographics Symposium on Rendering*, 43–54, 2005.
13. Sadiku, M. N., *Numerical Techniques in Electromagnetics*, 538–

541, CRC Press, 2001.

14. Schlick, C., "An inexpensive BRDF model for physically-based rendering," *Eurographics*, Vol. 13, No. 3, 234–246, 1994.
15. Didascalou, D., M. Döttling, T. Zwick, and W. Wiesbeck, "A novel ray optical approach to model wave propagation in curved tunnels," *IEEE Int. Veh. Technol. Conf. (VTC'99-Fall)*, 2313–2317, Amsterdam, The Netherlands, Sept. 1999.
16. Bang, J. K., B. C. Kim, S. H. Suk, K. S. Jin, and H. T. Kim, "Time consumption reduction of ray tracing for RCS prediction using efficient grid division and space division algorithms," *J. of Electromagn. Waves and Appl.*, Vol. 21, No. 6, 829–840, 2007.
17. Jin, K. S., T. I. Suh, S. H. Suk, B. C. Kim, and H. T. Kim, "Fast ray tracing using a space-division algorithm for RCS prediction," *J. of Electromagn. Waves and Appl.*, Vol. 20, No. 1, 119–126, 2006.
18. Tao, Y. B., H. Lin, and H. J. Bao, "kD-tree based fast ray tracing for RCS prediction," *Progress In Electromagnetics Research*, PIER 81, 329–341, 2008.
19. Liang, C., Z. Liu, and H. Di, "Study on the blockage of electromagnetic rays analytically," *Progress in Electromagnetics Research B*, Vol. No. 1, 253–268, 2008.
20. Teh, C. H. and H. T. Chuah, "An improved image-based propagation model for indoor and outdoor communication channels," *J. of Electromagn. Waves and Appl.*, Vol. 17, No. 1, 31–50, 2003.
21. Razavi, S. M. J. and M. Khalaj-Amirhosseini, "Optimization an anechoic chamber with ray-tracing and genetic algorithms," *Progress In Electromagnetics Research B*, Vol. 9, 53–68, 2008.
22. Liang, C., Z. Liu, and H. Di, "Study on the blockage of electromagnetic rays analytically," *Progress In Electromagnetics Research B*, Vol. 1, 253–268, 2008.
23. Wang, S., H. B. Lim, and E. P. Li, "An efficient ray-tracing method for analysis and design of electromagnetic shielded room systems," *J. of Electromagn. Waves and Appl.*, Vol. 19, No. 15, 2059–2071, 2005.
24. Chen, C. H., C. L. Liu, C. C. Chiu, and T. M. Hu, "Ultrawide band channel calculation by SBR/Image techniques for indoor communication," *J. of Electromagn. Waves and Appl.*, Vol. 20, No. 1, 41–51, 2006.